

# Maritime Aerosol Network as a component of AERONET



Observations and modeling of aerosol and clouds properties for climate studies

Workshop, 12-14 September 2011, Paris, France

## Maritime aerosol network as a component of AERONET – first results and comparison with global aerosol models and satellite retrievals

A. Smirnov<sup>1,2</sup>, B. N. Holben<sup>2</sup>, D. M. Giles<sup>1,2</sup>, I. Slutsker<sup>1,2</sup>, N. T. O'Neill<sup>3</sup>, T. F. Eck<sup>2,4</sup>, A. Macke<sup>5</sup>, P. Croo<sup>6</sup>, Y. Courcoux<sup>7</sup>, S. M. Sakerin<sup>8</sup>, T. J. Smyth<sup>9</sup>, T. Zielinski<sup>10</sup>, G. Zibordi<sup>11</sup>, J. I. Goes<sup>12</sup>, M. J. Harvey<sup>13</sup>, P. K. Quinn<sup>14</sup>, N. B. Nelson<sup>15</sup>, V. F. Radionov<sup>16</sup>, C. M. Duarte<sup>17</sup>, R. Losno<sup>18</sup>, J. Sciare<sup>19</sup>, K. J. Voss<sup>20</sup>, S. Kinne<sup>21</sup>, N. R. Nalli<sup>22</sup>, E. Joseph<sup>23</sup>, K. Krishna Moorthy<sup>24</sup>, D. S. Covert<sup>25</sup>, S. K. Gulev<sup>26</sup>, G. Milinevsky<sup>27</sup>, P. Larouche<sup>28</sup>, S. Belanger<sup>29</sup>, E. Horne<sup>30</sup>, M. Chin<sup>31</sup>, L. A. Remer<sup>32</sup>, R. A. Kahn<sup>32</sup>, J. S. Reid<sup>33</sup>, M. Schulz<sup>19</sup>, C. L. Heald<sup>34</sup>, J. Zhang<sup>35</sup>, K. Lapina<sup>34</sup>, R. G. Kleidman<sup>32,36</sup>, J. Griesfeller<sup>19</sup>, B. J. Gaitley<sup>37</sup>, Q. Tan<sup>4,31</sup>, and T. L. Diehl<sup>4,31</sup>

<sup>1</sup>Sigma Space Corporation, Lanham, Maryland, USA

<sup>2</sup>Biospheric Sciences Branch, NASA Goddard Space Flight Center, Greenbelt, Maryland, USA

<sup>3</sup>CARTEL, Université de Sherbrooke, Sherbrooke, Québec, Canada

<sup>4</sup>Goddard Earth Sciences and Technology Center, University of Maryland, Baltimore County, Baltimore, Maryland, USA

<sup>5</sup>Leibniz Institute for Tropospheric Research, Leipzig, Germany

<sup>6</sup>Leibniz Institute of Marine Sciences at the University of Kiel (IFM-GEOMAR), Kiel, Germany

<sup>7</sup>L'Observatoire de Physique de l'Atmosphère de la Réunion (OPAR), Université de la Réunion, Saint Denis de la Réunion, France

<sup>8</sup>Institute of Atmospheric Optics, Russian Academy of Sciences, Siberian Branch, Tomsk, Russia

<sup>9</sup>Plymouth Marine Laboratory, Plymouth, UK

<sup>10</sup>Institute of Oceanology, Polish Academy of Sciences, Sopot, Poland

<sup>11</sup>Institute for Environment and Sustainability, Joint Research Centre, European Commission, Ispra, Italy

<sup>12</sup>Bigelow Laboratory for Ocean Sciences, West Boothbay Harbor, Maine, USA

<sup>13</sup>National Institute of Water and Atmospheric Research, Wellington, New Zealand

<sup>14</sup>NOAA Pacific Marine Environmental Laboratory, Seattle, Washington, USA

<sup>15</sup>Institute for Computational Earth System Science, University of California, Santa Barbara, California, USA

<sup>16</sup>Arctic and Antarctic Research Institute, Saint Petersburg, Russia

<sup>17</sup>IMEDEA (CSIC-UIB), Instituto Mediterráneo de Estudios Avanzados, Esporles (Mallorca), Spain

<sup>18</sup>Laboratoire Interuniversitaire des Systèmes Atmosphériques, Université de Paris 7 et Université de Paris 12, Citeil, France

<sup>19</sup>Laboratoire des Sciences du Climat et de l'Environnement, Gif-sur-Yvette, France

<sup>20</sup>Physics Department, University of Miami, Coral Gables, Florida, USA

<sup>21</sup>Institute for Meteorology, University of Hamburg, Hamburg, Germany

<sup>22</sup>NOAA/NESDIS Center for Satellite Applications and Research (STAR), Camp Springs, Maryland, USA

<sup>23</sup>Department of Physics and Astronomy, Howard University, Washington, DC, USA

<sup>24</sup>Space Physics Laboratory, Vikram Sarabhai Space Centre, Trivandrum, India

<sup>25</sup>Department of Atmospheric Sciences, University of Washington, Seattle, Washington, USA

<sup>26</sup>P. P. Shirshov Institute of Oceanology, Russian Academy of Sciences, Moscow, Russia

<sup>27</sup>Space Physics Laboratory, Taras Shevchenko National University of Kyiv, Kyiv, Ukraine

<sup>28</sup>Institut Maurice-Lamontagne, Mont-Joli, Québec, Canada

<sup>29</sup>Département de biologie, chimie et géographie, Université du Québec à Rimouski, Rimouski, Québec, Canada

<sup>30</sup>Bedford Institute of Oceanography, Bedford, Nova Scotia, Canada

<sup>31</sup>Atmospheric Chemistry and Dynamics Branch, NASA Goddard Space Flight Center, Greenbelt, Maryland, USA

<sup>32</sup>Climate and Radiation Branch, NASA Goddard Space Flight Center, Greenbelt, Maryland, USA

<sup>33</sup>Marine Meteorology Division, Naval Research Laboratory, Monterey, California, USA

<sup>34</sup>Department of Atmospheric Science, Colorado State University, Fort Collins, Colorado, USA

<sup>35</sup>University of North Dakota, Grand Forks, North Dakota, USA

<sup>36</sup>Science Systems and Applications, Inc., Lanham, Maryland, USA

<sup>37</sup>Jet Propulsion Laboratory, California Institute of Technology, Pasadena, California, USA

Received: 21 December 2010 – Published in Atmos. Meas. Tech. Discuss.: 8 January 2011

Revised: 11 March 2011 – Accepted: 15 March 2011 – Published: 21 March 2011

Published by Copernicus Publications on behalf of the European Geosciences Union.

# Presenter – Alexander (Sasha) Smirnov



e-mail: [Alexander.Smirnov-1@nasa.gov](mailto:Alexander.Smirnov-1@nasa.gov)

Andrew Sayer, NASA/GSFC

Kostas Tsigaridis, NASA/GISS




GODDARD SPACE FLIGHT CENTER
+ Visit NASA.gov

# AERONET

## MARITIME AEROSOL NETWORK



+ AEROSOL OPTICAL DEPTH
+ AEROSOL INVERSIONS
+ SOLAR FLUX
+ OCEAN COLOR
+ MARITIME AEROSOL

+Home  
+AERONET Home

Maritime Aerosol

+ AEROSOL/FLUX NETWORKS

+ COLLABORATORS

+ DATA

+ NASA PROJECTS

+ PUBLICATIONS

+ STAFF

+ SYSTEM DESCRIPTION

MARITIME AEROSOL NETWORK (MAN)

The Maritime Aerosol Network (MAN) component of AERONET provides ship-borne aerosol optical depth measurements from the Microtops II sun photometers. These data provide an alternative to observations from islands as well as establish validation points for satellite and aerosol transport models. Since 2004, these instruments have been deployed periodically on ships of opportunity and research vessels to monitor aerosol properties over the World Oceans.



Microtops instruments currently in the network have five channels but they may have one of two configurations: 340, 440, 675, 870, 936nm or 440, 500, 675, 870, and 936nm. In addition, the instrument has built-in temperature and pressure sensors as well as the ability to log accurate time and geographical position using a GPS. The Microtops instruments are calibrated at the NASA Goddard Space Flight Center (GSFC) calibration facility via a transfer calibration procedure between the Microtops and the master Cimel sun photometer at GSFC, which has a calibration traceable to a Langley calibration of a Cimel sun photometer on Mauna Loa, Hawaii. In general, the estimated uncertainty of the aerosol optical depth in each channel does not exceed plus or minus 0.02, which is slightly higher than the uncertainty of AERONET field (not master) instruments.

Additional information on data processing and quality may be found by choosing the "Data" link in the left column.

**MAN Publication Reference:**

Smirnov, A., B. N. Holben, I. Slutsker, D. M. Giles, C. R. McClain, T. F. Eck, S. M. Sakerin, A. Macke, P. Croot, G. Zibordi, P. K. Quinn, J. Sciare, S. Kinne, M. Harvey, T. J. Smyth, S. Piketh, T. Zielinski, A. Proshutinsky, J. I. Goes, N. B. Nelson, P. Larouche, V. F. Radionov, P. Goloub, K. Krishna Moorthy, R. Matarrese, E. J. Robertson, and F. Jourdin (2009). **Maritime Aerosol Network as a component of Aerosol Robotic Network**, *J. Geophys. Res.*, 114, D06204, doi:10.1029/2008JD011257.

CRUISES



Level 1.5 | Level 2.0

The table below provides information for past, ongoing and planned cruises. The Ship column provides links to the information and data for each cruise. The Region column provides a KML file to view the cruise in Google Earth.

“It is very difficult, Sasha, to run free of charge network”

Dr. Michael King,  
January 2009

Year	Ship	Region	Status	2009	RP FLIP	Tropical Pacific	Completed	2011	RV Tangaroa	South Pacific Ocean	Completed
2004	RV Akademik Sergey Vavilov	Atlantic Ocean Transect, Southern Ocean	Completed	2009	RV Marion Dufresne	South Indian Ocean	Completed	2011	RV Melville	South Atlantic Ocean	Completed
2005-2006	RV Akademik Fedorov	Atlantic Ocean Transect, Antarctica	Completed	2009	RV Polarstern	Northern Greenland Sea	Completed	2011	RV Marion Dufresne	South Indian Ocean	Completed
2006-2007	RV Akademik Fedorov	Atlantic Ocean Transect, Antarctica	Completed	2009	RV Oceania	Baltic Sea	Completed	2011	FRV Tom Marshall	Moreton Bay	Completed
2007	Ecklonia	Atlantic Ocean near South African Coast	Completed	2009	RV Sonne	Pacific Ocean	Completed	2011	RV Astrolabe	Southern Ocean, South Pacific	Completed
2007	RV Polarstern	Atlantic Ocean Transect	Completed	2009	Trans Future 5	Pacific Ocean	Completed	2011	RV Melville	South Atlantic Ocean	Completed
2007	RV Urania	Mediterranean Sea	Completed	2009	RV Polarstern	Atlantic Ocean transect	Completed	2011	RV Challenger	coast of Tasmania	Completed
2007	Trans Future 5	Pacific Ocean Transect	Completed	2009	RV Antea	South Indian Ocean	Completed	2011	RRS Discovery	Tropical Atlantic	Completed
2007	RV Oceania	Baltic, Norwegian, Greenland Seas	Completed	2009	RRS James Cook	Atlantic Ocean transect	Completed	2011	RV Sagar Sampada	Arabian Sea	Completed
2007	RV Aranda	Gulf of Bothnia	Completed	2009	RV Akademik Ioffe	Atlantic Ocean transect	Completed	2011	RV Oceania	Baltic Sea	Completed
2007	CCGS Louis St. Laurent	Beaufort Sea	Completed	2009	RV Marion Dufresne	South Indian Ocean	Completed	2011	RV Laurence M. Gould	South Atlantic Ocean	Completed
2007	Roger Revelle	Arabian Sea	Completed	2009	RV Meteor	Tropical Atlantic	Completed	2011	RV Maria S. Merian	Tropical Atlantic	Completed
2007	RV Oceania	Baltic Sea	Completed	2009-2010	RV Marion Dufresne	South Indian Ocean	Completed	2011	RV Almirante Gago Coutinho	Atlantic Ocean	Completed
2007	Roger Revelle	Arabian Sea	Completed	2009-2010	RV Melville	South Pacific Ocean	Completed	2011	RV Oceania	Baltic Sea	Completed
2007	University of Bari	Adriatic Sea	Completed	2009-2010	RV Astrolabe	South Pacific and South Ocean	Completed	2011	RV Polarstern	Atlantic Ocean transect	Completed
2007	RV Polarstern	Atlantic Ocean Transect	Completed	2009-2010	RV Akademik Fedorov	Atlantic Ocean transect, South Ocean	Completed	2011	RV Oceania	Baltic Sea	Completed
2007	RRS Discovery	Canary-Cape Verde	Completed	2009-2010	RV Ocean Watch	Around the Americas	Completed	2011	KAUST Explorer	Red Sea	Completed
2007	RV Marion-Dufresne	South Indian Ocean	Completed	2010	Prince Albert II	Southern Atlantic and South Ocean	Completed	2011	RV Mare Nigrum	Black Sea	Completed
2007-2008	NOAA Ronald H. Brown	Pacific Ocean Transect	Completed	2010	RV Astrolabe	South Ocean	Completed	2011	RV Akademik	Black Sea	Completed
2007-2008	MV SA Agulhas	Southern Ocean	Completed	2010	FORV Sagar Sampada	Arabian Sea	Completed	2011	Dream Island	Red Sea	Completed
2007-2008	RV Akademik Fedorov	Atlantic Ocean Transect, Antarctica	Completed	2010	RV 1	South China Sea	Completed	2011	SRVx 8501	Chesapeake Bay	Completed
2008	RRS Discovery	Canary-Cape Verde	Completed	2010	CCGS Hudson	North Atlantic Ocean	Completed	2011	RV Akademik	Black Sea	Completed
2008	RV Polarstern	Southern Atlantic	Completed	2010	NOAA Ronald H. Brown	Tropical Atlantic	Completed	2011	NOAA Ronald H. Brown	Atlantic Ocean	Completed
2008	RV Knorr 2008	North Atlantic Ocean	Completed	2010	RV Southern Surveyor	Indian Ocean	Completed	2011	RV Oceania	Norwegian, Greenland Seas	Completed
2008	Trans Future 5	Pacific Ocean Transect	Completed	2010	RV Antea	Indian Ocean, Mozambique Channel	Completed	2011	EV Nautilus	Black, Mediterranean Seas	Ongoing
2008	RV L'Atalante	Gulf of Lion	Completed	2010	RV Marion Dufresne	Indian Ocean	Completed	2011	SY Task	Baltic Sea	Ongoing
2008	RV Polarstern	Atlantic Ocean Transect	Completed	2010	RV Polarstern	Atlantic Ocean transect	Completed	2011	RV Maria S. Merian	Atlantic Ocean	Ongoing
2008	MV Akbar 2008	Bay of Bengal	Completed	2010	NOAA Ronald H. Brown	Tropical Atlantic	Completed	2011	Trans Future 5	Pacific Ocean	Planned
2008	RV Islandia	Cape Verde	Completed	2010	MV Zim Iberia	Pacific Ocean, Indian Ocean, Arabian Sea	Completed	2011	RV Marion Dufresne	South Atlantic Ocean	Planned
2008	USCGC Healy	Bering Sea	Completed	2010	RV Oceania	Baltic Sea	Completed	2011	RV Mirai	Indian Ocean	Planned
2008	CCGS Amundsen	Beaufort Sea	Completed	2010	RV Atlantis	West Coast US	Completed	2011	RV Roger Revelle	Indian Ocean	Planned
2008	Trans Future 5	Pacific Ocean Transect	Completed	2010	RV Knorr	Tropical Atlantic	Completed				
2008	RP FLIP	Santa Barbara Basin	Completed	2010	RV Marion Dufresne	South China Sea, Sea of Japan	Completed				
2008	NRV Alliance	Ligurian Sea	Completed	2010	RV New Horizon	Gulf of California	Completed				
2008	RRS James Clark Ross	Atlantic Ocean Transect	Completed	2010	RV Melville	Tropical Pacific	Completed				
2008	RV Islandia	Cape Verde	Completed	2010	RV Marion Dufresne	Equatorial Pacific, Ceram Sea	Completed				
2008	NOAA Ronald H. Brown	Caribbean Sea, Pacific Ocean	Completed	2010	CCGS Amundsen	Labrador Sea, Hudson Bay	Completed				
2008	RV Polarstern	Atlantic Ocean transect	Completed	2010	RV Marion Dufresne	Indian Ocean	Completed				
2008	RV Maria S. Merian	Central and Tropical Atlantic	Completed	2010	RV Oceania	Norwegian, Greenland Seas	Completed				
2008	RV Marion-Dufresne	South Indian Ocean	Completed	2010	MV Zim San Diego	South China Sea, Gulf of Siam	Completed				
2008	RV Meteor	Pacific Ocean	Completed	2010	NRV Alliance	Ligurian Sea	Completed				
2008-2009	RV Sagar Kanya	Bay of Bengal	Completed	2010	RV Marion Dufresne	South Indian Ocean	Completed				
2008-2009	RV Akademik Fedorov	Atlantic Ocean transect	Completed	2010	RV Akademik Ioffe	Northern Atlantic	Completed				
2009	Norwegian Sun	Southern Atlantic and Pacific	Completed	2010	HC Maria	Atlantic Ocean	Completed				
2009	R/V Marcus G. Langseth	Tropical Pacific	Completed	2010	RV Marion Dufresne	South Indian Ocean	Completed				
2009	FORV Sagar Sampada	Arabian Sea	Completed	2010	RV Roger Revelle	North Pacific Ocean	Completed				
2009	RV Hesperides	Pacific Ocean	Completed	2010	RV Marion Dufresne	South Indian Ocean	Completed				
2009	NRV Alliance	Ligurian Sea	Completed	2010	RV Meteor	Tropical Atlantic	Completed				
2009	RV Oceania	Baltic Sea	Completed	2010	RRS Discovery	South Atlantic Ocean	Completed				
2009	RV Baruna Jaya IV	Java Sea	Completed	2010	RRS James Cook	Atlantic Ocean transect	Completed				
2009	RV Marion Dufresne	South Indian Ocean	Completed	2010	RV Polarstern	Atlantic Ocean transect	Completed				
2009	RV Polarstern	Atlantic Ocean Transect	Completed	2010	KAUST Explorer	Red Sea	Completed				
2009	RV Akademik	Black Sea	Completed	2010	RV Marion Dufresne	South Indian Ocean	Completed				
2009	RV Islandia	Cape Verde	Completed	2010	RRS James Cook	South Atlantic Ocean	Completed				
2009	RRS Discovery	Canary-Tropical Atlantic	Completed	2010	RV Southern Surveyor	Tasman Sea	Completed				
2009	RV Oceania	Baltic Sea	Completed	2010-2011	RRS James Clark Ross	South Atlantic Ocean	Completed				
2009	RV Jan Mayen	Norwegian, Greenland Seas	Completed	2010-2011	NP Almirante Maximiano	South Atlantic Ocean	Completed				
2009	RV Kilo Moana	North Pacific Ocean	Completed	2010-2011	RV Akademik Fedorov	Atlantic Ocean transect, Southern Ocean	Completed				
2009	NOAA Ronald H. Brown	Tropical Atlantic	Completed	2010-2011	RV Hesperides	Malaspina Expedition	Completed				
2009	RV Oceania	Norwegian, Greenland Seas	Completed	2011	RV Marion Dufresne	South Indian Ocean	Completed				
2009	CCGS Amundsen	Beaufort Sea	Completed	2011	RV Kilo Moana	North Pacific Ocean	Completed				

icy and Important Notices



Curator: David M. Giles  
 NASA Official: Brent N. Holben  
 Last Updated: July 16, 2009

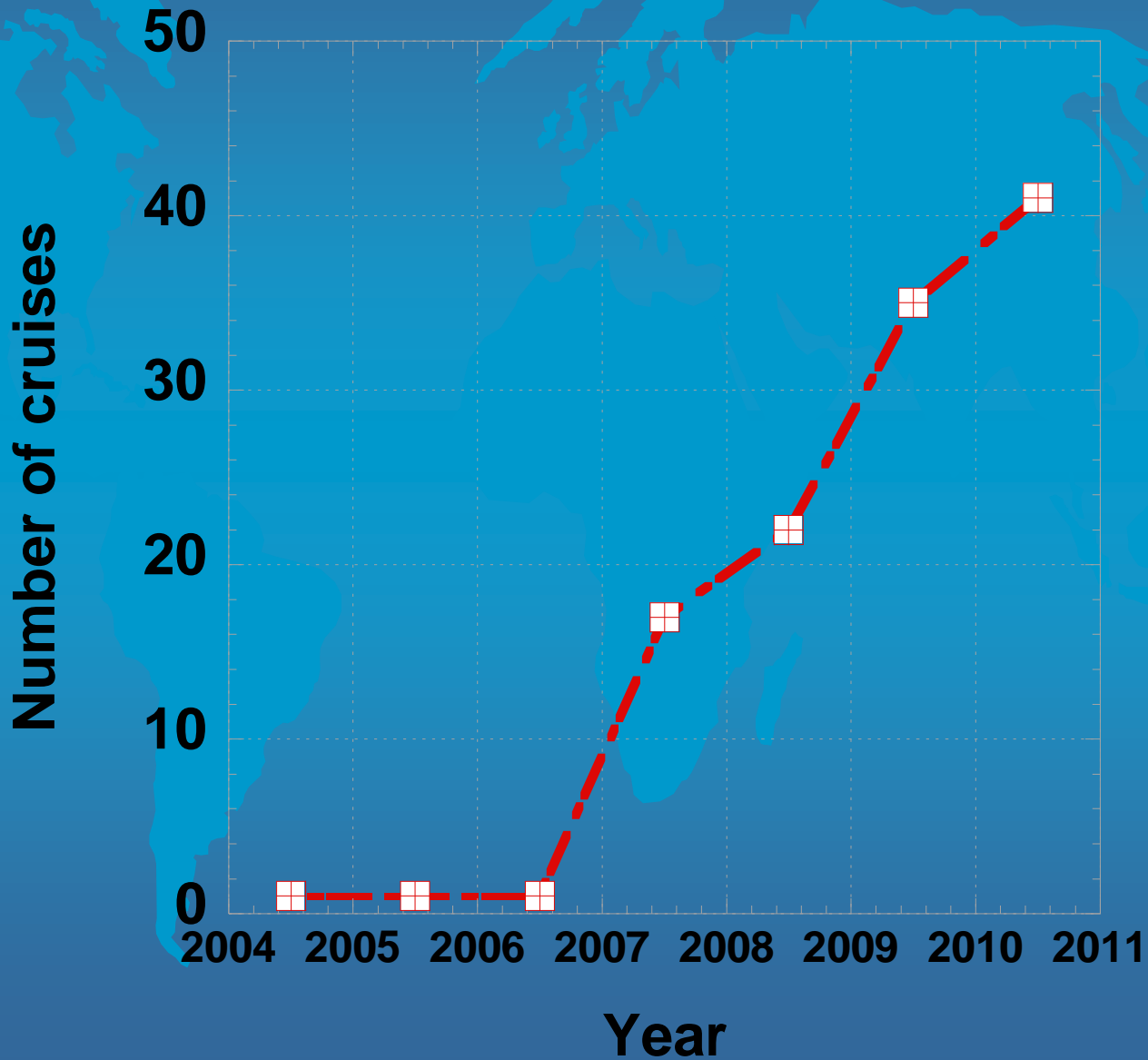


# Scientific Objectives



- **Climate change studies (direct and indirect forcing)**
- **Satellite retrievals validation**
- **Validation of global aerosol transport model simulations**
- **Filling data gaps in global aerosol distribution**
- **How representative are the island measurements**
- **Atmospheric correction**

# Number of cruises completed



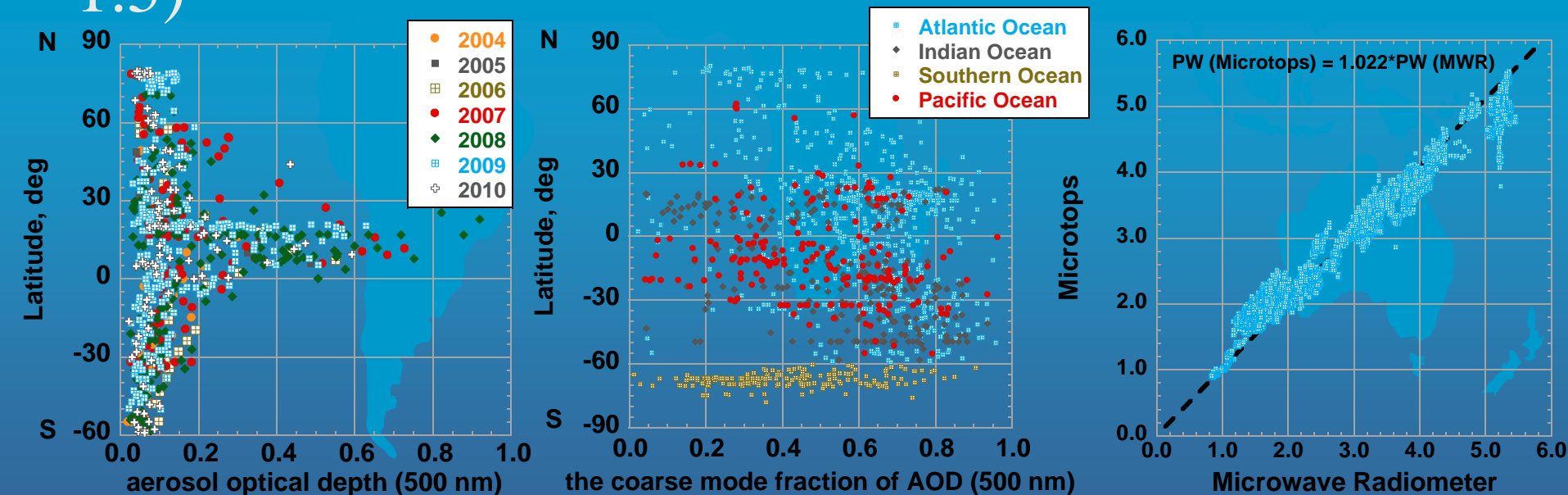


# Summary

- Number of cruises completed – 145
- Number of measurement days → 2600
- Number of measurement series → 15600
- Number of ongoing cruises – 3
- Number of planned cruises - 7

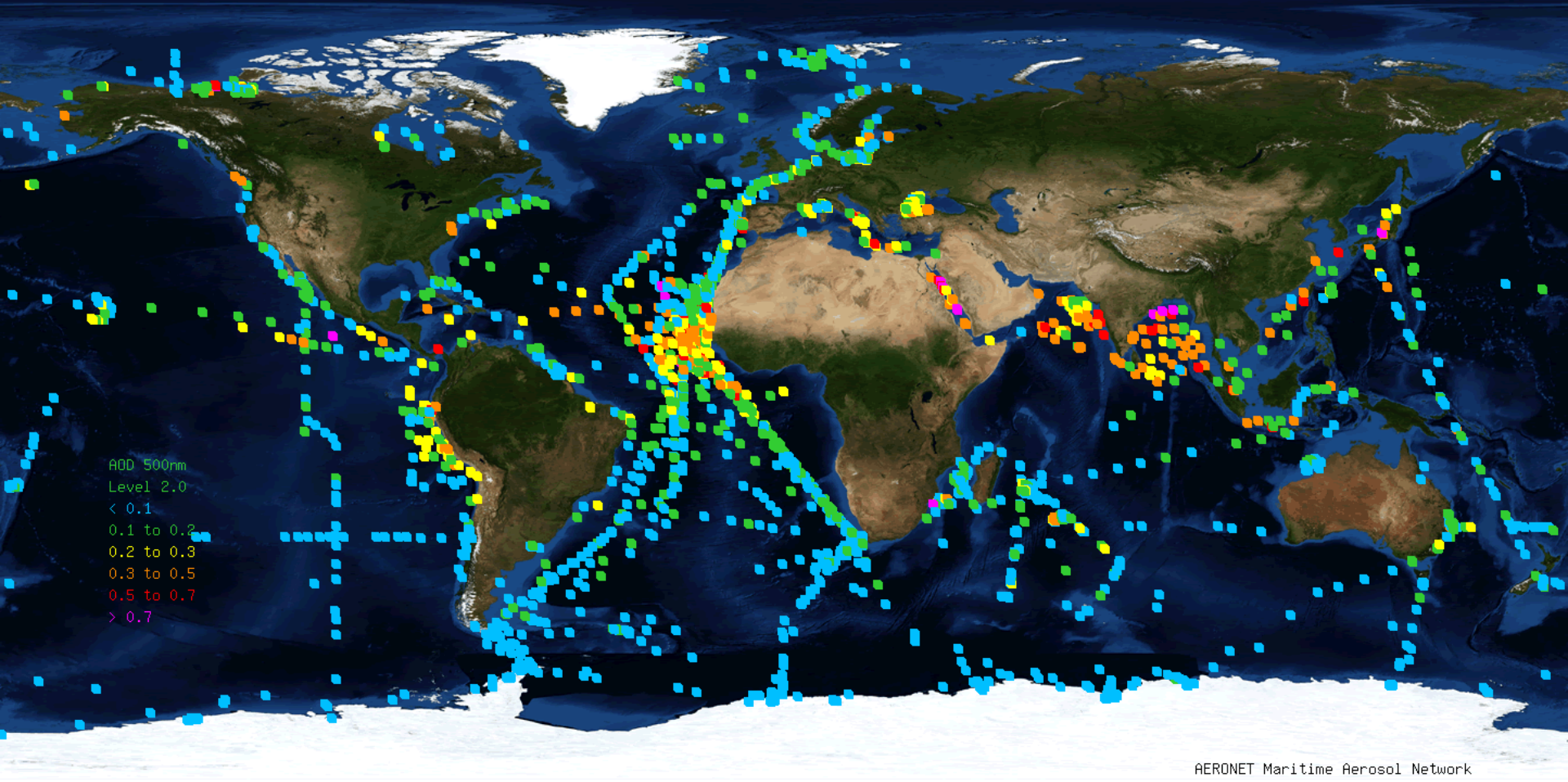
# MAN products:

- Aerosol optical depth (Level 1; Level 1.5; Level 2)
- Water vapor content (Level 1; Level 1.5; Level 2)
- Aerosol optical depths: fine (sub-micron) and coarse (super-micron) at 500 nm (Level 1; Level 1.5)



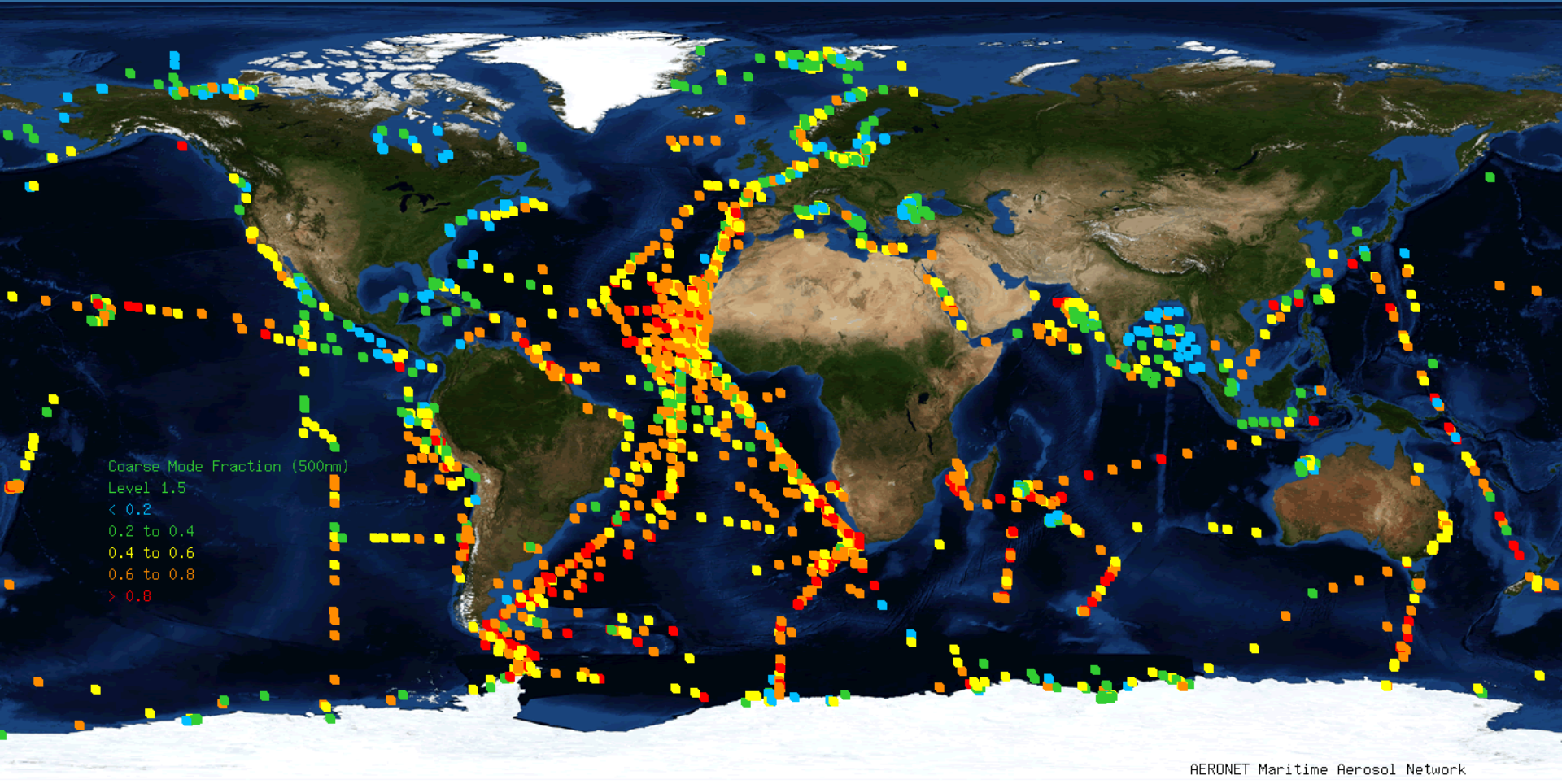


# Maritime Aerosol Network global coverage (September 2011)



Cruise tracks and daily averages of aerosol optical depth at 500 nm (squares are colored with respect to AOD values, i.e. **blue** –  $AOD < 0.10$ , **green** –  $0.1 \leq AOD < 0.2$ , **yellow** –  $0.2 \leq AOD < 0.3$ , **orange** –  $0.3 \leq AOD < 0.5$ , **red** –  $0.5 \leq AOD < 0.7$ , **purple** –  $AOD \geq 0.7$ ).

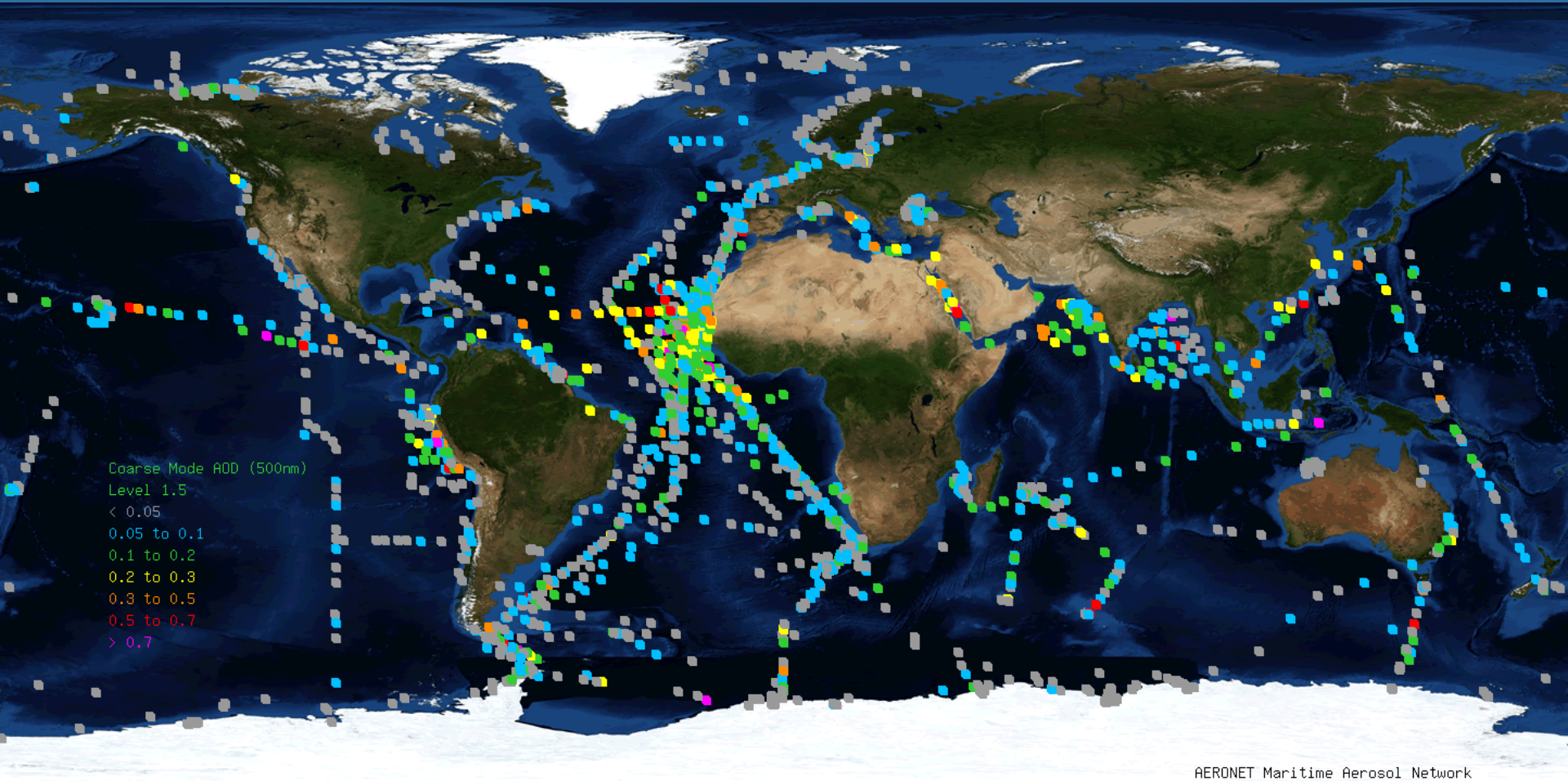
# Coarse mode fraction of AOD



Cruise tracks and daily averages of coarse mode fraction of aerosol optical depth at 500 nm (squares are colored with respect to coarse mode fraction, i.e. **blue** –  $cmf < 0.2$ , **green** –  $0.2 \leq cmf < 0.4$ , **yellow** –  $0.4 \leq cmf < 0.6$ , **orange** –  $0.6 \leq cmf < 0.8$ , **red** –  $cmf > 0.8$ ).

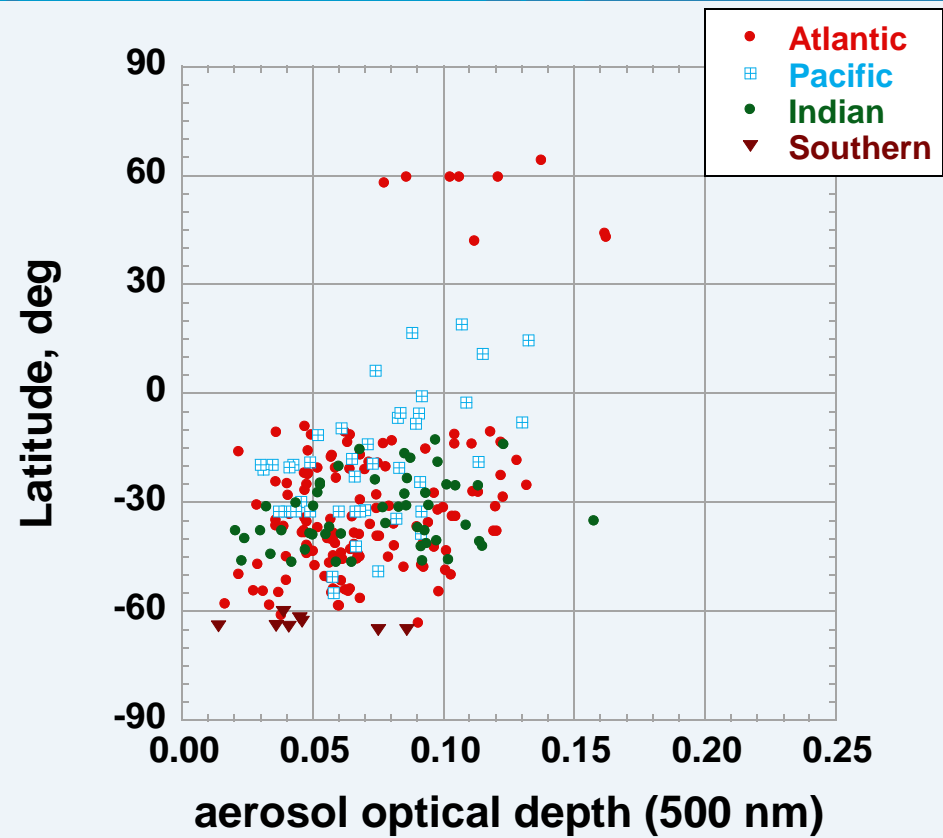
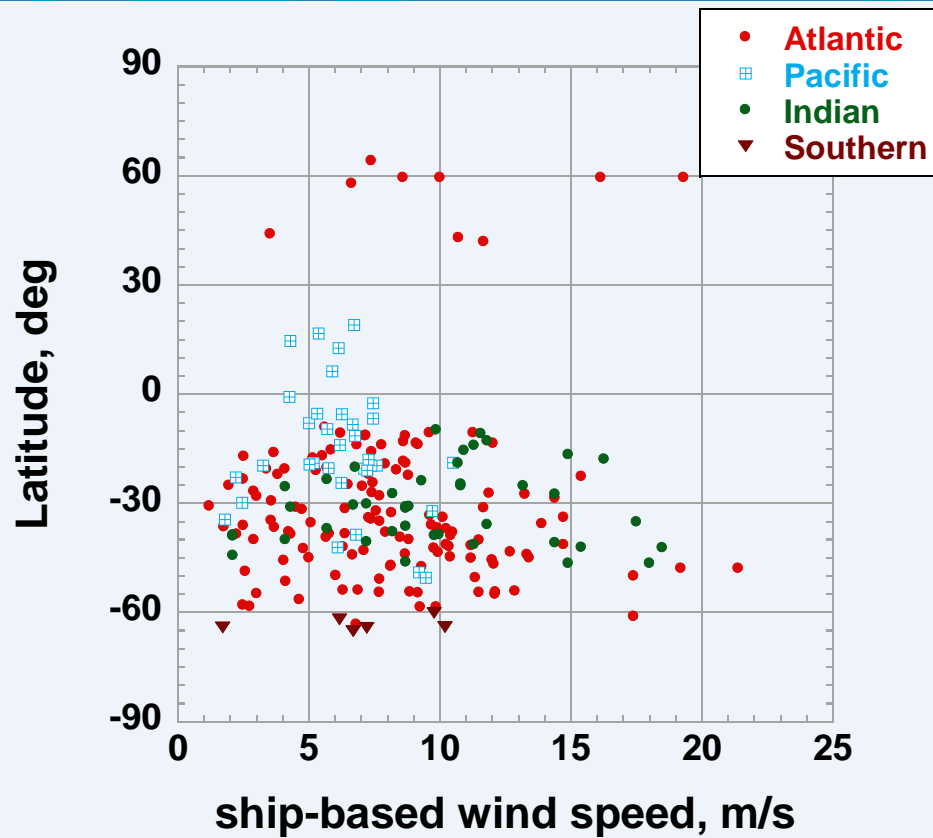


# Coarse mode AOD

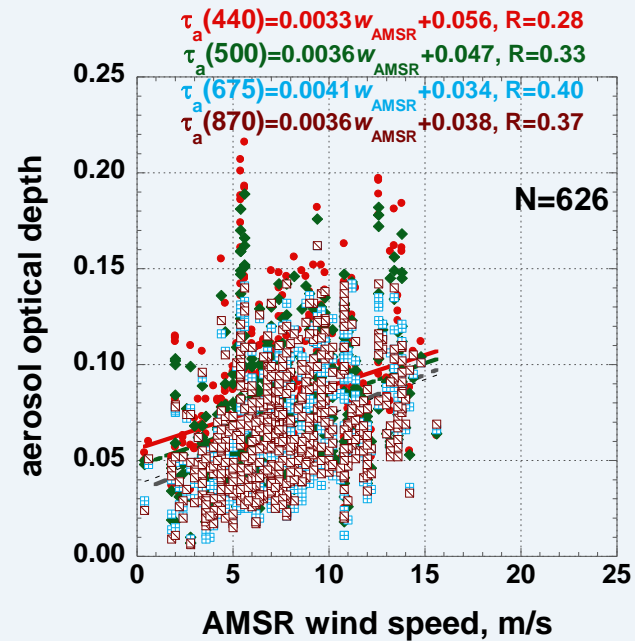
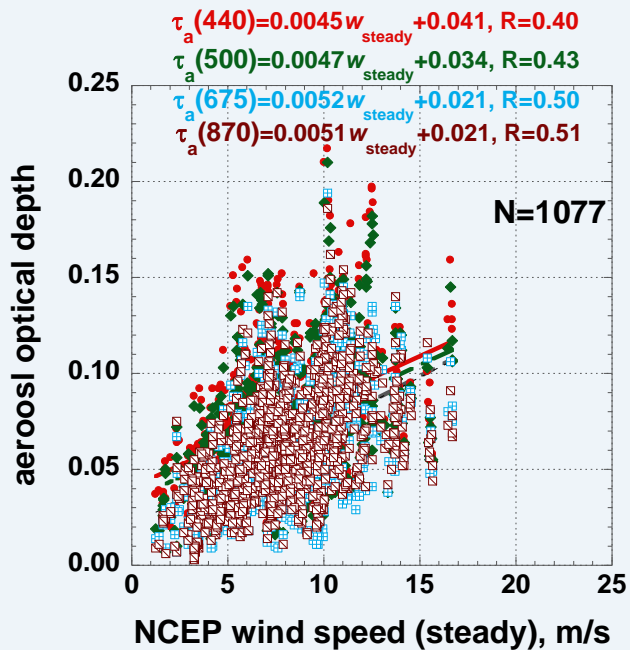
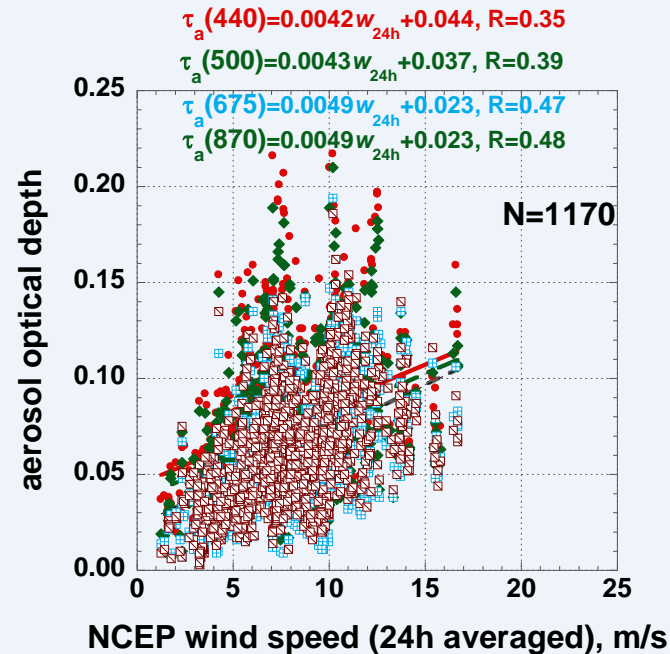
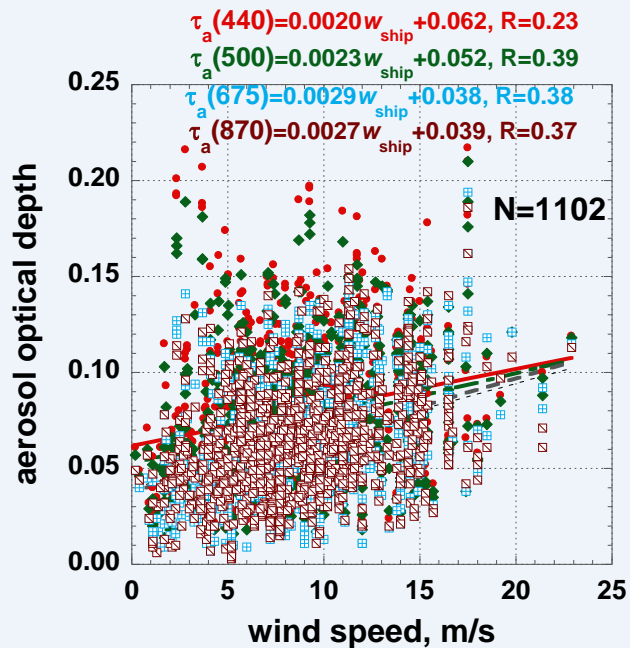


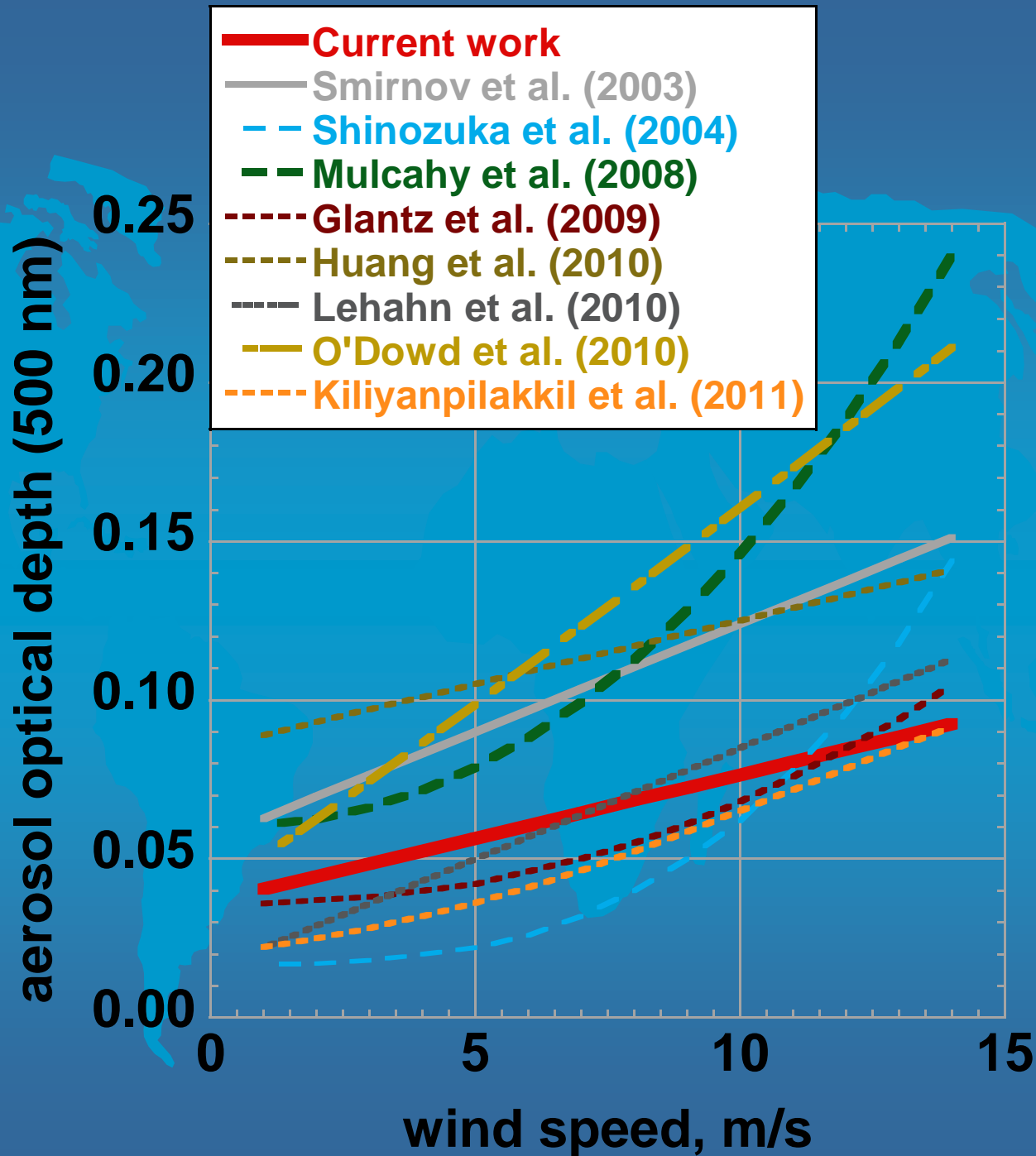
Cruise tracks and daily averages of coarse mode aerosol optical depth at 500 nm (squares are colored with respect to coarse AOD values, i.e. grey –  $AOD < 0.05$ , blue –  $0.05 < AOD < 0.10$ , green –  $0.1 \leq AOD < 0.2$ , yellow –  $0.2 \leq AOD < 0.3$ , orange –  $0.3 \leq AOD < 0.5$ , red –  $0.5 \leq AOD < 0.7$ , purple –  $AOD \geq 0.7$ ).

# AOD and wind speed analysis





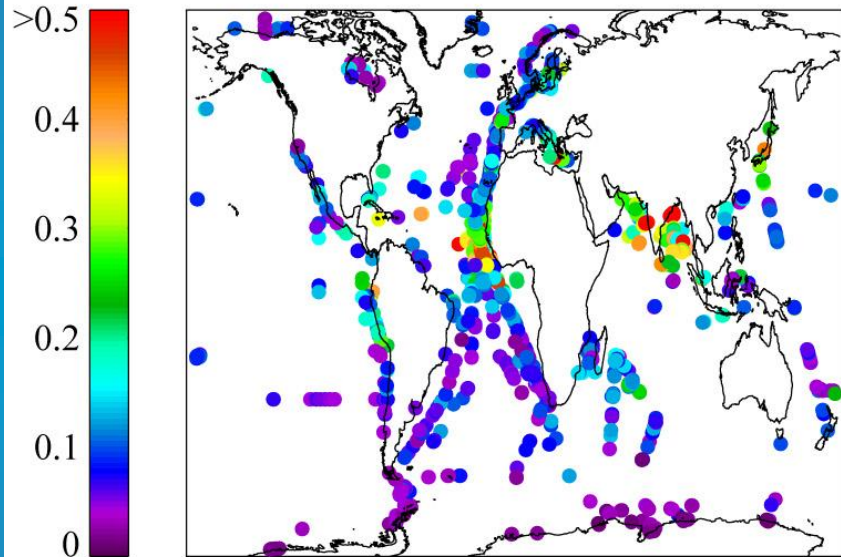




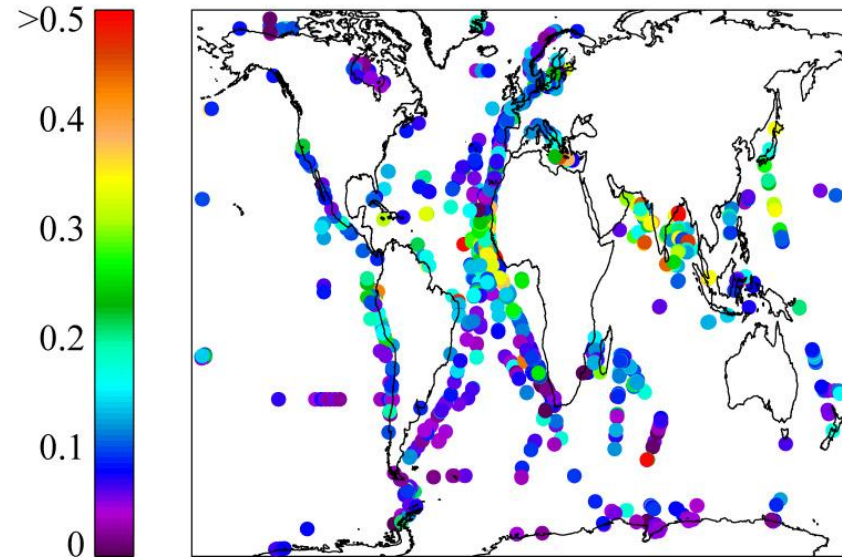


# Comparison with satellite retrievals

MAN 550 mn AOD

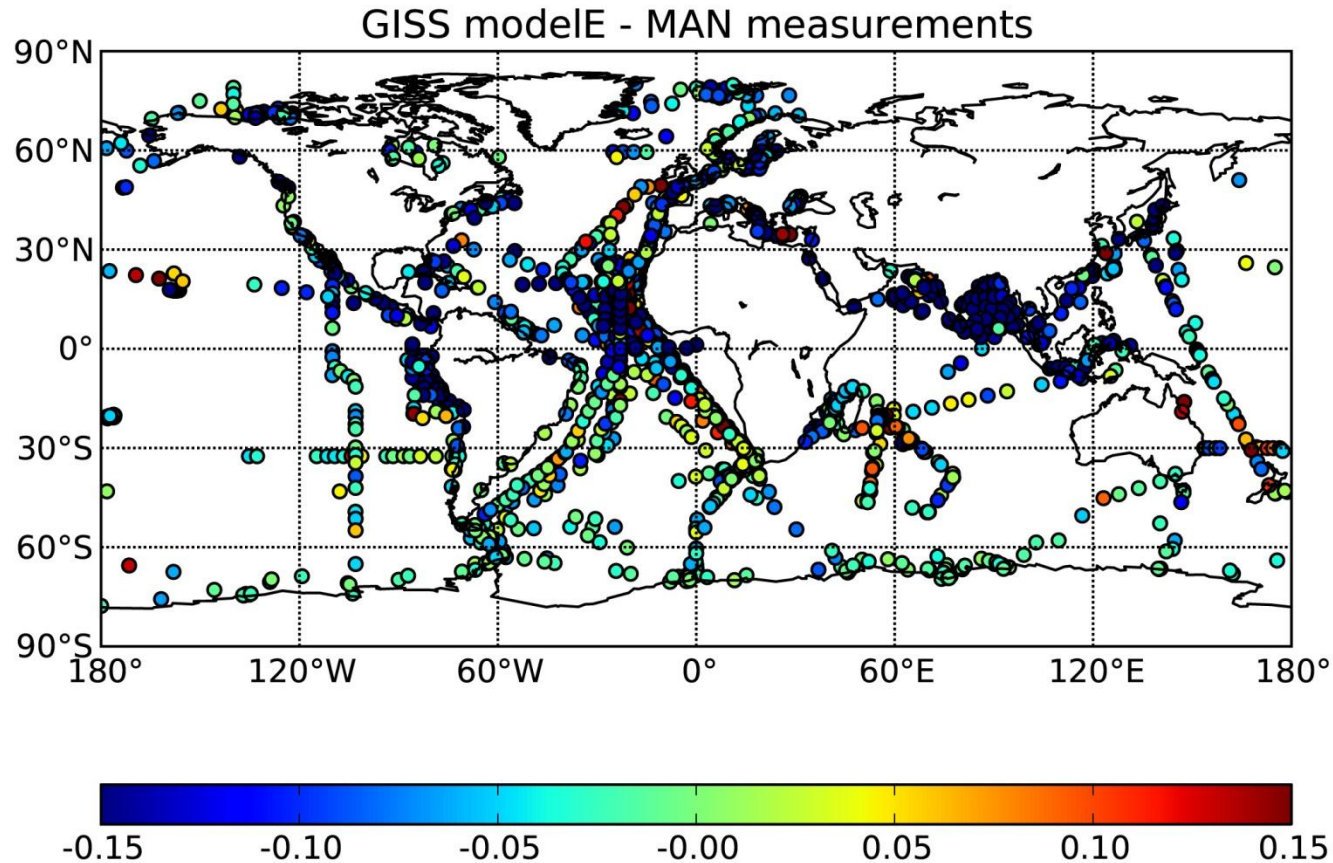


SeaWiFS 550 mn AOD



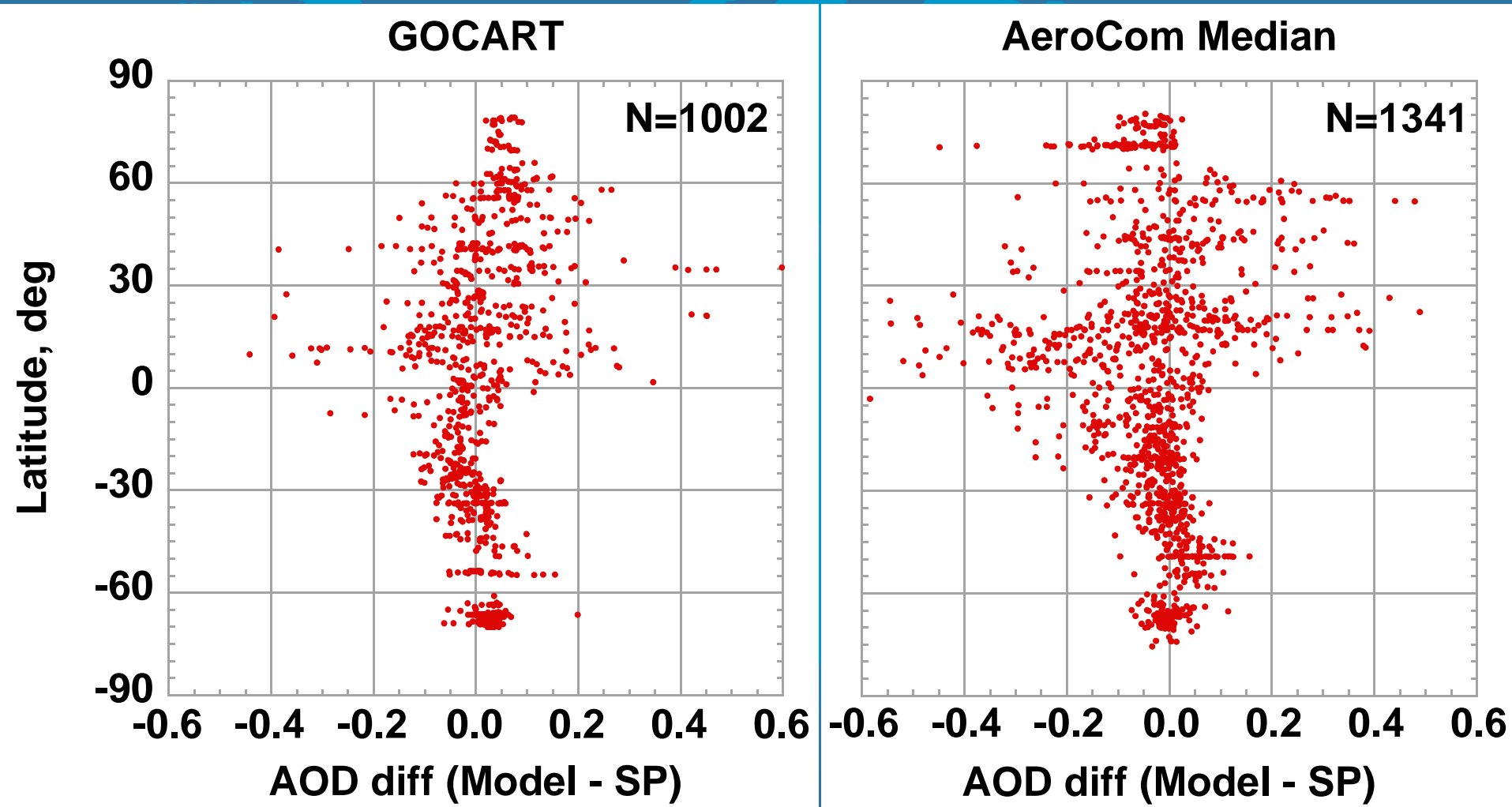
Courtesy Andrew Sawyer, NASA/GSFC

# Comparison with global aerosol model



Courtesy Kostas Tsigaridis, NASA/GISS

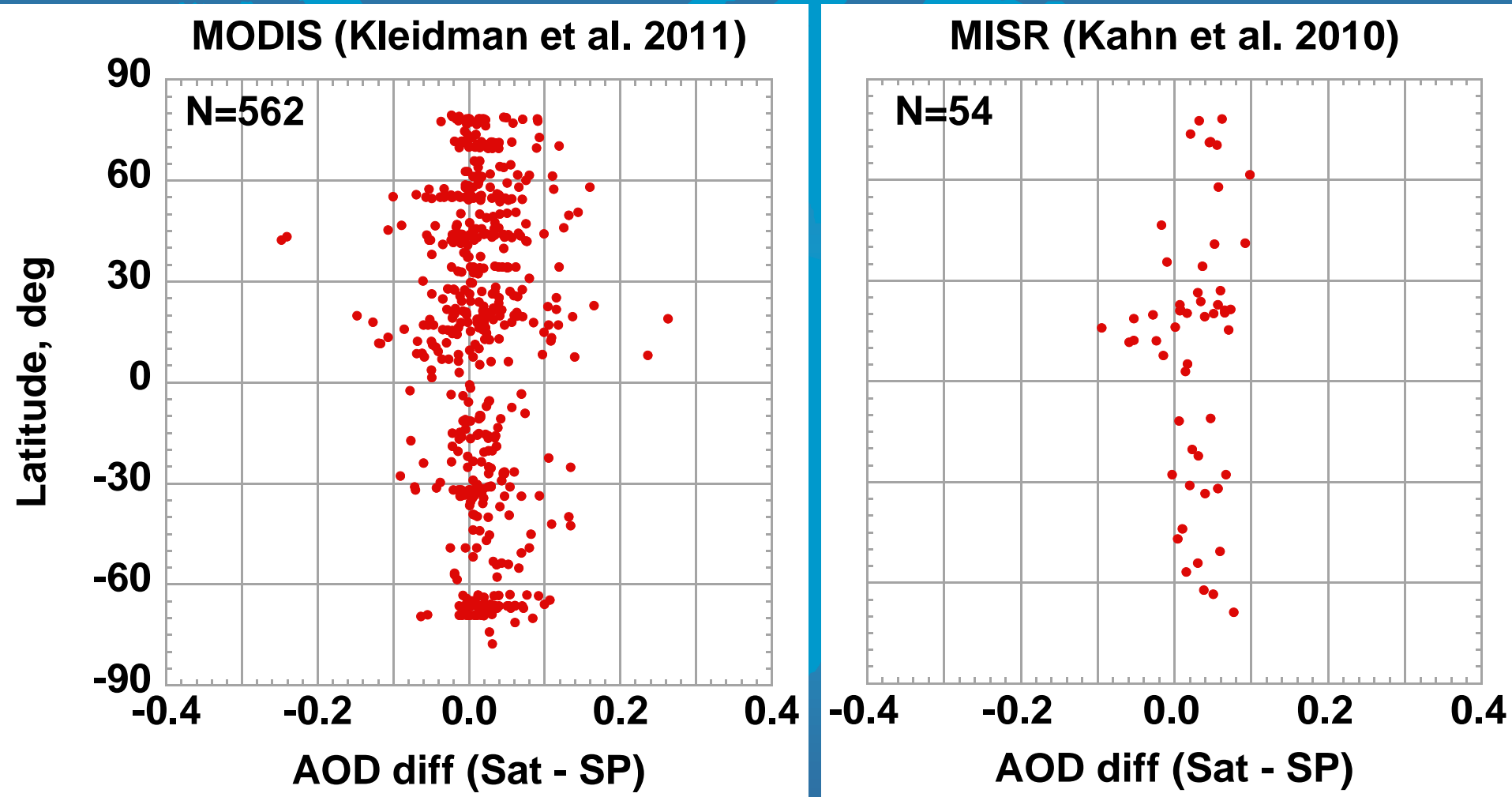
# Comparison with global aerosol models



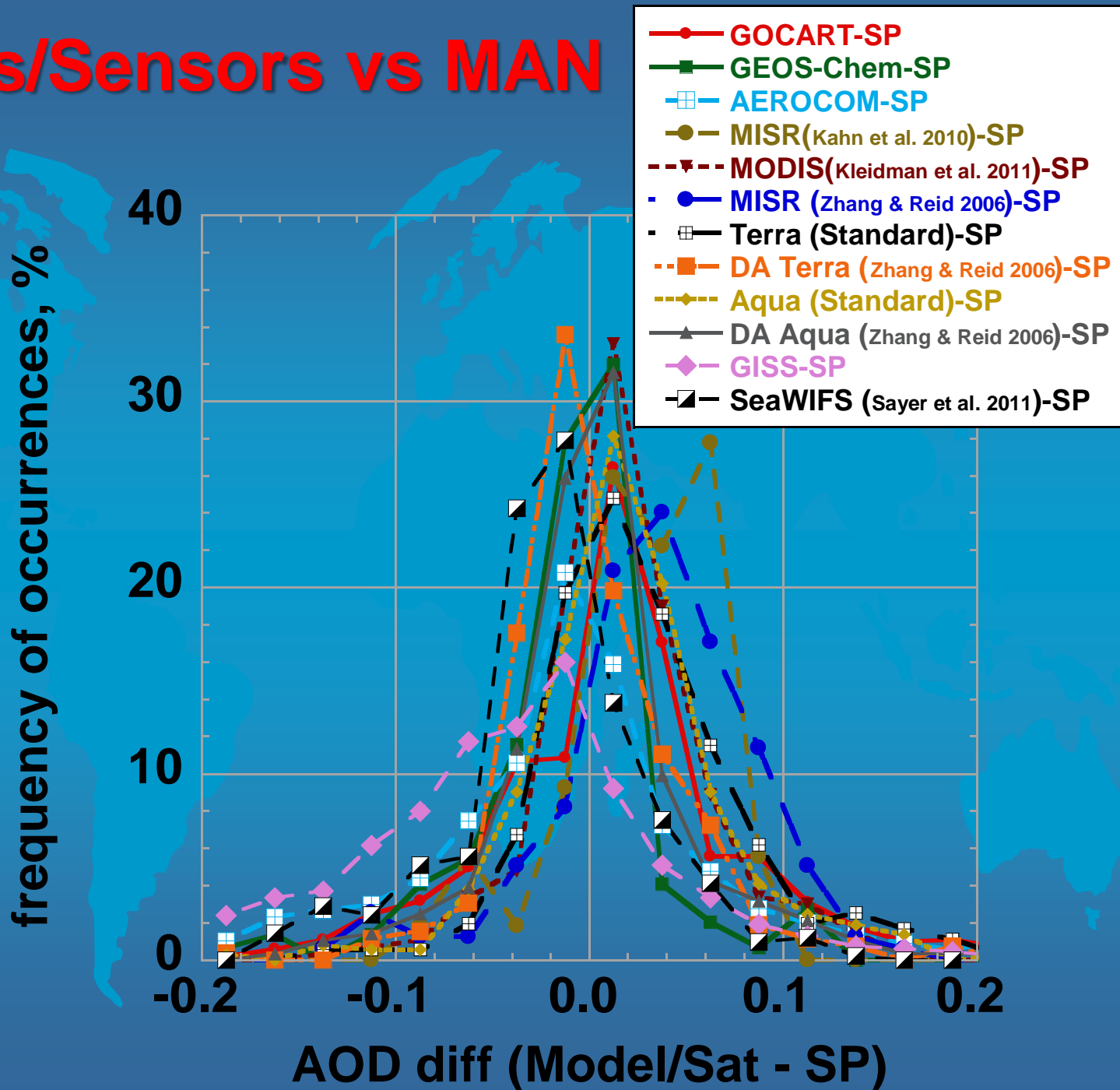
Smirnov et al., Maritime Aerosol Network as a component of AERONET – first results and comparison with global aerosol models and satellite retrievals, *Atmos. Meas. Tech.*, 4, 583–597, 2011.



# Comparison with satellite retrievals



# Models/Sensors vs MAN



# Tom Tans and his role in the Aeronet

JOURNAL OF GEOPHYSICAL RESEARCH, VOL. 106, NO. D11, PAGES 12267-12297, JUNE 16, 2001

## An emerging ground-based aerosol climatology: Aerosol optical depth from AERONET

B. N. Holben,<sup>1</sup> T. Tans,<sup>2</sup> A. Smirnov,<sup>3</sup> T. F. Eck,<sup>1,4</sup> I. Slutsker,<sup>5</sup> N. Ahnhanou,<sup>6</sup> W. W. Newcomb,<sup>7</sup> J. S. Schafer,<sup>1,4</sup> B. Charette,<sup>8</sup> F. Lavenu,<sup>9</sup> Y. J. Kaufman,<sup>10</sup> J. Vande Castle,<sup>11</sup> A. Setzer,<sup>12</sup> B. Markham,<sup>13</sup> D. Clark,<sup>12</sup> R. Frouin,<sup>14</sup> R. Halthore,<sup>1,15</sup> A. Karnel,<sup>16</sup> N. T. O'Neill,<sup>17</sup> C. Pietras,<sup>18</sup> R. T. Pinker,<sup>19</sup> K. Voss,<sup>20</sup> and G. Zibordi<sup>21</sup>

**Abstract.** Long-term measurements by the AERONET program of spectral aerosol optical depth, precipitable water, and derived Angstrom exponent were analyzed and compiled into an aerosol optical properties climatology. Quality assured monthly means are presented and described for primary sites and 21 additional midlayer sites with distinct aerosol regimes representing tropical biomass burning, boreal forests, midlatitude biomass, midlatitude dry climates, oceanic sites, desert sites, and background sites. Seasonal trends for each of these sites are discussed and climatic averages presented.

### 1. Introduction

Man is altering the aerosol environment through land cover change, combustion of fossil fuels, and the introduction of particulates and gas species to the atmosphere. Each perturbation has some impact on the aerosol environment. How much aerosol man is contributing to the atmosphere is not known. Even more fundamental, do we not know the current level of aerosol loading that we have no definitive measure of change for future assessment (Endrey, 1994). Regardless of current conditions, the extent of local aerosol perturbations on a global scale is the subject of extensive ground level, airborne and satellite research (Kaufman et al., 1997; King et al., 1999). Investigations have been initiated by concerns ranging from radiative forcing by aerosols, long-term impacts on climate and public health, natural and ecological impacts, as well as the future of sea level habitations and political interests.

Seasonal trends for each of these sites are discussed and climatic averages presented. Aerosol optical loading that we have no definitive measure of change for future assessment (Endrey, 1994). Regardless of current conditions, the extent of local aerosol perturbations on a global scale is the subject of extensive ground level, airborne and satellite research (Kaufman et al., 1997; King et al., 1999). Investigations have been initiated by concerns ranging from radiative forcing by aerosols, long-term impacts on climate and public health, natural and ecological impacts, as well as the future of sea level habitations and political interests. Seasonal trends for each of these sites are discussed and climatic averages presented.

Copyright 2001 by the American Geophysical Union. Paper number 2001JD001411. DOI: 10.1029/2001JD001411

## AERONET—A Federated Instrument Network and Data Archive for Aerosol Characterization

B. N. Holben,<sup>1</sup> T. F. Eck,<sup>1</sup> I. Slutsker,<sup>1</sup> D. Tans,<sup>2</sup> J. P. Bur,<sup>3</sup> A. A. Setzer,<sup>4</sup> E. Vermote,<sup>5</sup> J. A. Reagan,<sup>6</sup> Y. J. Kaufman,<sup>7</sup> T. Nakajima,<sup>8</sup> F. Lavenu,<sup>9</sup> I. Jankovic,<sup>10</sup> and A. Smirnov<sup>11</sup>

The concept and description of a remote sensing aerosol monitoring network initiated by NASA, developed to support NASA, CNRS, and NASA's Earth orbiting system under the name AERONET and expanded by national and international collaborations is described. Recent development of aerosol-resistant automatic sun and sky viewing spectral radiometers enable frequent measurements of atmospheric aerosol optical properties and precipitable water at remote sites. Transmission of minute measurements to the ground via commercial GDS and METEOSAT Data Collection Systems allows reception and processing in near real time from approximately 75% of the Earth's surface and with the expected addition of GMS, the coverage will increase to 90% to 100%. NASA developed a UNIX-based real-time processing, display and analysis system providing internet access to the emerging global database information on the system is available on the project homepage, <http://aeronet.gsfc.nasa.gov>. The philosophy of an open access database, operational processing, and a user-friendly interface has contributed to the growth of international cooperation for ground-based aerosol monitoring and support of a number of other projects.

<sup>1</sup>NASA/Goddard Space Flight Center, Greenbelt, Maryland; <sup>2</sup>NASA/CIRES, Colorado State University, Fort Collins, Colorado; <sup>3</sup>NASA/GSFC, Greenbelt, Maryland; <sup>4</sup>NASA/GSFC, Greenbelt, Maryland; <sup>5</sup>NASA/GSFC, Greenbelt, Maryland; <sup>6</sup>NASA/GSFC, Greenbelt, Maryland; <sup>7</sup>NASA/GSFC, Greenbelt, Maryland; <sup>8</sup>NASA/GSFC, Greenbelt, Maryland; <sup>9</sup>NASA/GSFC, Greenbelt, Maryland; <sup>10</sup>NASA/GSFC, Greenbelt, Maryland; <sup>11</sup>NASA/GSFC, Greenbelt, Maryland.

Address correspondence to Bill Holben, NASA/GSFC, Code 6102, NASA/GSFC, Greenbelt, MD 21051. E-mail: holben@gsfc.nasa.gov

JOURNAL OF GEOPHYSICAL RESEARCH, VOL. 106, NO. D11, PAGES 12267-12297, JUNE 16, 2001

## Retrieval of aerosol optical thickness and size distribution over ocean from the MODIS airborne simulator during TARPOX

D. Tans,<sup>1</sup> L. A. Remar,<sup>2</sup> Y. J. Kaufman,<sup>3</sup> S. Mintov,<sup>4</sup> P. V. Hobbs,<sup>5</sup> J. M. Livingston,<sup>6</sup> P. B. Russell,<sup>7</sup> A. Smirnov,<sup>8</sup>

**Abstract.** Radiation and in situ measurements collected during the Tropospheric Aerosol Radiation Fielding Observation Experiment (TARPOX) are used to test the method for retrieval of aerosol optical properties and loading from MODIS. MODIS is a satellite-based Earth Radiation Budgeting Satellite to be launched in 1998 aboard the first EOS Earth Observing Satellite. Following the MODIS pre-launch test, the retrieval of aerosol optical thickness and size distribution (integrated over the ocean is a wide spectral range (0.55–2.13 μm)) and the retrieval of aerosol optical thickness (proportional to the aerosol loading) and aerosol size distribution (integrated over the vertical column of the medium (unpolarized) aerosol) are compared to ground-based measurements. The LST includes the phase-scattering accumulation mode, cloud-phase accumulation mode, and a coarse mode that is represented by aerosol particles (aerol) and dust. In each iteration, one accumulation and one coarse mode can be retrieved. The inversion retrieves the ratio of the contribution to the optical thickness of the two particle modes and the mean particle size that best fits the measurements. The algorithm is successfully applied to the data sets acquired during TARPOX. The MODIS airborne simulator (MAS) aboard the NASA DC-8 aircraft flew several times during the experiment. The MODIS data are compared to the ground-based measurements. The MODIS data are compared to the ground-based measurements. The MODIS data are compared to the ground-based measurements.

Copyright 2001 by the American Geophysical Union.



GSFC, 31 July 1998

**Introduction.** Interest in global aerosol monitoring has increased recently following the recognition that their contributions to atmospheric and Earth processes are very important. Since frequent and global coverage of the Earth's atmosphere is achievable only by observations from space, efforts have been made to develop new satellite-based instruments for monitoring key aerosol parameters by observations from space. Early studies (Junge, 1957; Phin, 1976; McFar et al., 1973; Collins, 1975; Eckart and Chetani, 1976; Aronin et al., 1983) showed the potential of visible satellite imagery to detect aerosols over oceans. Because of the limited number of channels on the initial instruments used for GDS and Meteosat, and two channels for AVHRR/NOAA, three algorithms can derive only the total aerosol loading.



JOURNAL OF GEOPHYSICAL RESEARCH, VOL. 106, NO. D11, PAGES 1645-1664, JUNE 1, 2001

## Relationship between column aerosol optical thickness and in situ ground based dust concentrations over Barbados

A. Smirnov,<sup>1</sup> B. N. Holben,<sup>1</sup> D. Savoie,<sup>2</sup> J. M. Prospero,<sup>3</sup> Y. J. Kaufman,<sup>4</sup> D. Tans,<sup>5</sup> T. F. Eck,<sup>6</sup> I. Slutsker<sup>7</sup>

**Abstract.** Aerosol optical depth measurements over Barbados during six winters within the spectral range 400–1020 nm. Optical depth above a prescribed marine stratus with a maximum obscuration of 0.2. The temporal trend in dust concentration was also examined. A simple linear regression model has been established between near monthly values of aerosol optical depth and dust concentrations (measured in micrograms per cubic meter). The regression coefficient is 0.03. Using the extension of optical depth for any specific time period, when dust concentration measurements are available. The goodness of the regression was Barbados used as dust source and high humidity was a problem during the measurement period. However, we found strong correlation between visibility and performance were satisfactory. Table 1 presents the deployment and calibration history. Throughout the whole measurement period the 460 nm channel at 1000 nm the calibration history was reliable except for a month in 1998. The 870 nm channel was considered to be reliable on 400 days. During 1996 and 9 months of 1997 (217 days) the 670 nm channel was damaged as a result of a lightning strike. The 670 nm channel was repaired and recalibrated. The 670 nm channel was repaired and recalibrated. The 670 nm channel was repaired and recalibrated.

### Introduction

Knowledge of aerosol characteristics on a global scale, their diurnal change and interrelations with other atmospheric parameters is of great importance if we are to understand the mechanisms which control the aerosol optical depth of the atmosphere. One of the major goals of the Global Aerosol Climatology Project (GACP) is a systematic application of aerosol retrieval algorithms to the whole period of available satellite measurements (Carnot et al., 1996). Retrieved aerosol optical parameters should be validated employing ground-based measurements (Carnot et al., 1996). Retrieved aerosol optical parameters should be validated employing ground-based measurements (Carnot et al., 1996). Retrieved aerosol optical parameters should be validated employing ground-based measurements (Carnot et al., 1996).

### Data Collection

An automatic sun and sky viewing radiometer (CAMEL) was installed at an Arnono Radiosonde Network (ARONET) site on Barbados, Barbados. The CAMEL instrument was installed at an Arnono Radiosonde Network (ARONET) site on Barbados, Barbados. The CAMEL instrument was installed at an Arnono Radiosonde Network (ARONET) site on Barbados, Barbados.

Copyright 2001 by the American Geophysical Union.

Copyright 2001 by the American Geophysical Union.





la vie est dure  
les femmes coutent chères  
et les enfants arrivent trop faciles

life is tough  
women are expensive  
and children come too easy



ЛИТЕРАТУРА

1. Смирнов А. В., Шифрин К. С. Статистика спектральной прозрачности атмосферы над морем.— В кн.: Физика пограничного слоя атмосферы и ее прикладные аспекты. Л., 1984, с. 121—127. (Сб. науч. трудов (межвузовский); Вып. 85).
2. Волков Б. П., Волгин В. М., Ершов О. А. Спектрофотометр для изучения оптических характеристик морского аэрозоля.— В кн.: Оптика моря. М.: Наука, 1983. 246 с.
3. Шифрин К. С., Ершов О. А., Волгин В. М., Кокорин А. М. Исследование аэрозоля над морем по данным береговых наблюдений.— Изв. АН СССР. Физика атмосферы и океана, 1980, № 3, с. 254—260.
4. Elterman L. UV, visible and IR attenuation for altitudes to 50 km.— Env. Res. Pap., 1968, № 285, p. 50.
5. Шифрин К. С., Минин П. И. К теории негоризонтальной видимости.— Тр. ГГО, 1957, вып. 68, с. 5—75.
6. Таварткиладзе К. А. Статистические характеристики спектральной оптической толщины атмосферы над морской поверхностью.— Изв. АН СССР. Физика атмосферы и океана, 1979, № 11, с. 1218—1222.
7. Малевич М. С., Георгиевский Ю. С., Чавро А. П., Шукуров А. Х. Статистические характеристики спектральной структуры ослабления радиации в приземном слое воздуха.— Изв. АН СССР. Физика атмосферы и океана, 1977, № 12, с. 1257—1267.
8. Viollier M., Tanpe' D., Dechamps P. An algorithm for remote sensing of water colour from space.— Bound. Layer Met., 1980, v. 18, № 3, p. 247—267.

Ленинградское отделение  
Института океанологии  
им. П. П. Ширшова АН СССР  
Ленинградский  
гидрометеорологический  
институт

Поступила в редакцию  
1.XI.1984

OPTICAL DEPTH OF ATMOSPHERIC AEROSOL OVER THE SEA

SHIFRIN K. S., VOLGIN V. M., VOLKOV B. N.,  
ERSHOV O. A., SMIRNOV A. V.

The results are given of measuring the optical depths of the atmospheric aerosol obtained in marine and coastal regions. Despite significant changeability of the optical depths of the atmospheric aerosol they were shown to have good correlation in the visible and near infrared spectral bands. Regression relations are given which may be used in the problems of remote sensing the ocean — atmosphere system.

Относительная ошибка  $\Delta = \frac{\delta_{\lambda_k}}{\bar{\tau}_a(\lambda_k)}$  составляет около 20%. Погрешности между измеренными и рассчитанными  $\tau_a$  иллюстрирует рис. 1.

Анализ собственных чисел и собственных векторов ковариационной матрицы показал, что два первых собственных числа дают 97% вклада в среднюю по спектру дисперсию (92 и 5% соответственно). Поэтому два собственных вектора  $\varphi_1(\lambda)$  и  $\varphi_2(\lambda)$  удовлетворительно описывают спектральную структуру аэрозольной оптической толщи (с<sub>i</sub> — коэффициенты разложения):

$$\tau_a(\lambda) = \bar{\tau}_a(\lambda) + \sum_{i=1}^2 c_i \varphi_i(\lambda). \quad (4)$$

Значения  $\varphi_1(\lambda)$  и  $\varphi_2(\lambda)$  приведены в табл. 5.

Вектор  $\varphi_1(\lambda)$  повторяет спектральный ход  $\sigma(\lambda)$ . Вектор  $\varphi_2(\lambda)$  меняет знак около 520 нм. Как показано в [7],  $\varphi_1(\lambda)$  характеризует знакопостоянные вариации  $\Delta\tau_a(\lambda) = \tau_a(\lambda) - \bar{\tau}_a(\lambda)$ , а  $\varphi_2(\lambda)$  описывает те реализации  $\tau_a(\lambda)$ , для которых  $\Delta\tau_a(\lambda)$  меняют знак в области 520 нм.

Изменчивость  $\tau_a(\lambda)$  зависит от изменчивости концентрации и от изменчивости структуры аэрозоля, т. е. от  $f(a)$ . Введем отношение

$$\epsilon = \tau_a(439) / \tau_a(660).$$

В алгоритме исключения влияния атмосферы при определении концентрации хлорофилла в морской воде, предложенном в [8], величина  $\epsilon$  считается заданной. Реальная изменчивость  $\epsilon$  представлена в табл. 6. Как следует из табл. 6, коэффициенты вариации  $V_\epsilon$  не превышают 18%, в то время как  $V_{\tau_a} \sim 40-60\%$ . Таким образом, концентрационная изменчивость  $\tau_a(\lambda)$  заметно больше структурной.

Рассмотрим теперь величину параметра Ангстрема  $\alpha$ . Для океанских данных среднее значение его оказалось 0,55, а для всех данных 0,61. Коэффициент вариации  $V_\alpha = 0,51$ . Из табл. 4 видно, что в океанских условиях параметр  $\alpha$  меньше в районах с более прозрачной атмосферой. Увеличение общей мутности атмосферы обычно сопровождается подъемом кривой  $\tau_a(\lambda)$  в ультрафиолетовой области. Это приводит к возрастанию  $\alpha$ .

На рис. 2 приведен частотный график  $\alpha$  при  $\Delta\alpha = 0,1$ . Два ярко выраженных максимума, по-видимому, характеризуют два типа «оптической погоды» в атмосфере над морем. Значению  $\alpha = 0,45$  соответствует  $\bar{\tau}_a = 0,18$ , которое близко к «стандартному». Величина  $\alpha = 0,95$  характеризует замутненную атмосферу, здесь  $\bar{\tau}_a = 0,30$ . Отметим, что на рис. 2 намечается появление третьего максимума в области  $\alpha$  около 0,1. Добавим, что среднее значение  $\bar{\alpha} = 0,98$  при  $\bar{\tau}_a = 0,41$  было получено в [8] в результате годичного мониторинга аэрозольной оптической толщины на Азорских островах (там  $N = 182$ ).

Общая тенденция в поведении  $\tau_a(\lambda)$  такова, что в условиях прозрачной атмосферы преобладает квазинейтральный ход (малые  $\alpha$ ); с увеличением мутности показатель  $\alpha$  растет, проходит через максимум и при туманной дымке снова стремится к нулю. Это означает, что в морской атмосфере малому  $\alpha$  соответствуют как случаи малых, так и случаи весьма больших  $\tau_a$ .

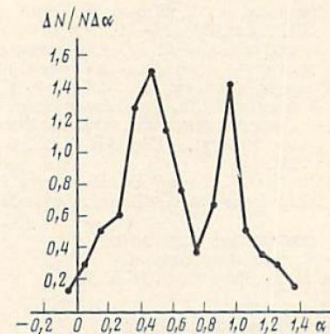


Рис. 2. Частотный график показателя Ангстрема  $\alpha$



УДК 551.510.42 : 551.521.31

## ОПТИЧЕСКАЯ ТОЛЩИНА АЭРОЗОЛЯ В ХАРАКТЕРНЫХ МОРСКИХ РЕГИОНАХ

ВОЛГИН В. М., ЕРШОВ О. А., СМИРНОВ А. В., ШИФРИН К. С.

Сообщаются результаты измерений аэрозольных оптических толщин в видимой и близкой ИК-областях спектра в различных районах Мирового океана. Показано, что статистически различимы только три характерных региона: 1) области открытого океана, 2) прибрежные районы (вместе с внутренними морями), 3) «море мрака». Анализ спектрального хода аэрозольной оптической толщины показал, что данные наблюдений различаются по величине в центре видимой области и по параметру Ангстрема. Результаты анализа и установленные статистические связи могут быть использованы в качестве априорной информации в задачах дистанционного зондирования.

1. Аэрозольная оптическая толщина  $\tau_a$ , ее спектральный ход  $\tau_a(\lambda)$  представляют собой важную характеристику атмосферы над океаном. Знание ее необходимо при дистанционном зондировании океана из космоса. К сожалению, до сих пор не принесли успеха попытки найти устойчивые корреляционные связи между  $\tau_a$  и метеопараметрами на уровне моря. Поэтому вопрос о возможности косвенного определения  $\tau_a$  по метеоданным остается открытым. В связи с этим важную роль продолжают играть различные регрессионные и эмпирические соотношения, позволяющие с той или иной точностью определять  $\tau_a(\lambda)$  через какие-либо измеряемые характеристики. Величина  $\tau_a(\lambda)$  зависит от множества разных, плохо контролируемых факторов. Один из способов решения задачи об определении  $\tau_a(\lambda)$  состоит в получении достаточного эмпирического материала и установлении подходящих статистических связей. Такие связи позволят нам по одному или нескольким значениям  $\tau_a(\lambda_i)$  при некоторых  $\lambda_i$  рекомендовать наиболее вероятные значения  $\tau_a$  при всех других  $\lambda$  или рекомендовать стандарты  $\tau_a(\lambda)$ , которые можно использовать в тех или иных регионах, вообще не делая никаких измерений, и т. д. Некоторые результаты в этом направлении были опубликованы ранее [1—3].

В настоящей работе приведены данные новых измерений  $\tau_a(\lambda)$ , проводившихся в 1985—1986 гг., и указаны их статистические характеристики. Мы рассмотрим также совокупность всех данных, новых и старых, для выяснения возможности их классификации по типичным регионам (различающимся механизмом генерации аэрозоля). Покажем, что уверенно выделяются три характерных региона: 1) открытый океан, 2) прибрежные районы, куда попадают наблюдения во внутренних морях и береговые измерения, 3) тропическая зона Атлантического океана, подверженная влиянию сахарских выносов (так называемое «море мрака»). Хотя количество значений, относящихся к каждой из этих групп данных, заметно меньше общего числа измерений за счет выигрыша в однородности материала, статистические связи в целом оказываются менее размытыми.

2. Статистические характеристики новых данных приведены в табл. 1. Аппаратура и методика измерения изложена в [1], где показано также,

которую первую первые собственные числа вносят в суммарную по спектру дисперсию. Видно, что первые два вектора удовлетворительно описывают спектральную структуру  $\tau_a(\lambda)$  для прибрежных измерений. В случае океанской атмосферы можно также пользоваться двумя собственными векторами, но здесь сумма первых двух собственных чисел вносит в суммарную дисперсию почти такой же вклад, что одно число для прибрежной выборки.

Векторы  $\varphi_1(\lambda)$  имеют схожий между собой и с [1] спектральный ход для всех районов. Вектор  $\varphi_2(\lambda)$  меняет знак один раз, но для океанской выборки его спектральный ход несколько отличается от остальных. Это связано, по-видимому, с немонотонностью спектрального хода  $\tau_a(\lambda)$  и  $r_{\tau\tau}(\lambda_i, \lambda_k)$  из-за ошибок измерений.

Результаты измерений в океанских, прибрежных районах и «море мрака» позволяют сделать следующие выводы.

1. Оптическое состояние атмосферы в каждом регионе следует характеризовать двумя параметрами: значением  $\tau_a(550)$  и параметром Ангстрема  $\bar{\alpha}$ . Первый характеризует величину замутнения, а второй — среднюю спектральную изменчивость  $\tau_a(\lambda)$  в изучаемом спектральном диапазоне.

2. Атмосфера над океаном существенно (более чем в 2 раза) прозрачнее атмосферы других регионов. Среднеквадратичные отклонения также в 4—5 раз меньше.

3. Установлены регрессионные соотношения между  $\tau_a$  в синей и красной областях спектра, которые могут быть использованы в алгоритмах исключения влияния атмосферы.

4. Показано, что для моделирования особенностей спектрального хода  $\tau_a(\lambda)$  в морской атмосфере достаточно использовать два собственных вектора.

Авторы благодарят Б. Н. Волкова за помощь в проведении измерений.

### ЛИТЕРАТУРА

1. Шифрин К. С., Волгин В. М., Волков Б. Н., Ершов О. А., Смирнов А. В. Оптическая толщина аэрозоля атмосферы над морем//Исследования Земли из космоса. 1985. № 4. С. 21—30.
2. Ершов О. А., Смирнов А. В. Спектральная прозрачность прибрежной атмосферы//Исследования Земли из космоса. 1986. № 5. С. 3—8.
3. Смирнов А. В., Шифрин К. С. Статистика спектральной прозрачности атмосферы над морем//Физика пограничного слоя атмосферы и ее прикладные аспекты: Межуз. сб. научн. тр. Л., 1984. Вып. 85. С. 121—127.
4. Prodi F., Tomasi C. Sahara dust program//J. Aerosol Sci. 1983. V. 14. № 4. P. 517—527.
5. Кондратьев К. Я., Бартенева О. Д., Васильев О. Б. и др. Аэрозоль в районе АТЭП и его радиационные свойства//Тр. ГГО. 1976. Вып. 381. С. 67—130.
6. Шифрин К. С., Минин И. Н. К теории негоризонтальной видимости//Тр. ГГО. 1957. Вып. 68. С. 5—75.
7. Гашко В. А., Шифрин К. С. Спектральная прозрачность атмосферы в северо-западной части Тихого океана//Оптика моря. М.: Наука, 1983. С. 190—194.
8. Viollier M., Tahre D., Dechamps P. An algorithm for remote sensing of water colour from space//Boundary Layer Meteorol. 1980. V. 18. № 3. P. 247—267.

Ленинградский  
гидрометеорологический ин-т,  
Ленинградский отдел  
Ин-та океанологии АН СССР

Поступила в редакцию  
29.X.1987



## Saharan Aerosols over the South of France: Characterization Derived from Satellite Data and Ground Based Measurements

J. L. DEUZE, C. DEVAUX, M. HERMAN, R. SANTER AND D. TANRE

Laboratoire d'Optique Atmosphérique, Université des Sciences et Techniques de Lille, France

20 May 1987 and 28 September 1987

### ABSTRACT

In July 1983, the summer transport of Saharan aerosols across the Mediterranean Sea was observed. The dust cloud was particularly dense and was clearly detected in A.V.H.R.R. and METEOSAT imageries. Optical thicknesses and Angström coefficients have been derived from these pictures. During the same period, ground based observations—transmission, aureole and polarization measurements—were performed at the Observatoire de Haute Provence (southeast of France). Measured aerosol optical thicknesses at 550 nm were as large as about 1.5.

The optical thicknesses and Angström coefficients derived from the two experiments are compared and are in good agreement.

### 1. Introduction

In summertime, westward migrations of saharan dust clouds over the tropical North Atlantic Ocean are commonly observed from satellite imagery. Local and time variations of the dust have been described by Carlson and Prospero (1972). The aerosol optical thickness has been derived from satellite data in the visible range (Carlson et al. 1977; Norton et al. 1980; Griggs 1979; Koepke and Quenzel 1979). The integrated mass of dust was obtained by Fraser (1976). Dust outbreaks have also been observed over the eastern Mediterranean Sea by Mekler et al. (1977) and Otterman et al. (1982). These dust clouds have also appeared during nighttime in the METEOSAT IR channel (Legrand et al. 1985).

During July 1983, ground based measurements were planned at the O.H.P. ("Observatoire de Haute Provence", about 80 km from the mediterranean coast with an altitude of 1900 m) in order to observe the El Chichon stratospheric layer. This objective was disturbed by the occurrence of a saharan dust outbreak, which provided the opportunity to characterize this dust cloud from ground measurements.

This event was looked for in the AVHRR (on NOAA-7) and METEOSAT imageries over the Mediterranean Sea. Thus, we have the interesting possibility of comparing aerosol characterization derived from satellite imagery with a more detailed characterization derived from ground observations. We will show that

the aerosol thickness ( $\tau_a$ ) and the Angström coefficient deduced from satellite data are in good agreement with the ground measurements.

### 2. The ground based measurements

#### a. Presentation of the measurements, from 26 July to 29 July 1983

Extinction measurements were performed with two multispectral radiometers. The first one has a silicium detector and covers the range from 440 to 1100 nm; the second has a PbS detector, and performs measurements up to 3000 nm. The two radiometers had been previously calibrated, (April 1983), using Langley plots. The seven band measurements are centered at 445, 551, 648, 864, 1040, 1586 and 2208 nm.

In the wavelength range of our band measurements, water vapor and ozone absorption is simply a corrective term. This gaseous absorption was merely computed from LOWTRAN-5 code (Kneizys et al. 1980), by using the climatologic value of London et al. (1976) for the ozone content, and the midlatitude summer model of Mc Clatchey et al. (1970) for the water vapor content. The Rayleigh optical thickness was estimated from the pressure measurements. By subtracting Rayleigh scattering and gaseous absorption components from the total optical thickness, we obtained the aerosol optical thickness  $\tau_a$ . Figure 1 gives  $\tau_a$  versus the UTC time, at  $\lambda = 550$  nm, for the 4 observation days. On the morning of 26 July, the aerosol content was almost constant and Langley plots drawn from these data confirmed the previous calibration. Despite the high altitude of the site (1900 m),  $\tau_a$  was always very large, with a maximum of 1.7 on 27 July, which is quite an un-

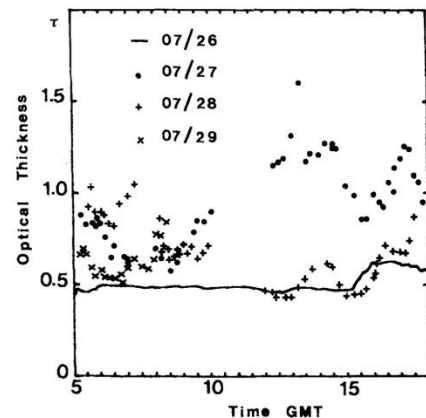


FIG. 1. Instantaneous aerosol optical thickness  $\tau_a$ , at 550 nm, for the 4 days. A full line has been drawn through the smooth measurements obtained on 26 July. The symbols for other days are included on the figure. It was initially planned that the traditional Langley technique would be used to derive  $\tau_a$ , so that no extinction measurements were performed around noon, when the air mass did not vary; this explains the lack of information, from 1000 to 1300 UTC, in Fig. 1.

usual value. Note that it is unlikely that cirrus clouds could explain these large values of  $\tau_a$ . The sky was routinely observed around the sun disk, using cross-

polaroids in order to attenuate the sun irradiance, and no cirrus clouds were observed during the campaign.

The spectral dependence of the aerosol optical thickness,  $\tau_a(\lambda)$ , proved to be nearly constant for a given day, but exhibited large variations from day to day. Figure 2 shows the  $\tau_a(\lambda)$  behavior observed for the 4 days. On 27 July, the aerosol optical thickness increased largely in the blue range. For the other days, the spectral variation was more flat, mainly on 29 July where the optical thickness was almost constant in the visible range, and decreased slowly at near-IR wavelengths. Figure 2 shows that, through the large investigated spectral range, the  $\tau_a(\lambda)$  behavior could not be accounted for with a single Angström coefficient. Therefore, the log-log plots of  $\tau_a(\lambda)$  versus  $\lambda$ , in Fig. 2, were crudely fitted by two linear laws, from 445 to 668 nm and from 668 to 1650 nm, thus providing two Angström coefficients, hereafter noted  $\alpha_v$  and  $\alpha_{IR}$ , respectively. In Table 1, we reported for the 4 days the values obtained for  $\alpha_v$  and  $\alpha_{IR}$ . The large value of  $\alpha_v$  proves the presence of small particles on 27 July, whereas larger particles were predominant on 29 July. The mean deviations  $\Delta\alpha_v$  (or  $\Delta\alpha_{IR}$ ) (see Table 1) showed fairly good stability of the aerosol size distribution for a given day, as noted previously. Deviations of the Angström coefficients were somewhat larger in near-IR than in the visible, as a result of the larger measurement errors.

Aureole measurements were performed at  $\lambda = 850$  nm, using a silicium detector with an aperture angle of  $1^\circ$ . About 5 min were needed to scan scattering angles from  $2^\circ$  to  $30^\circ$ ; the observations were performed

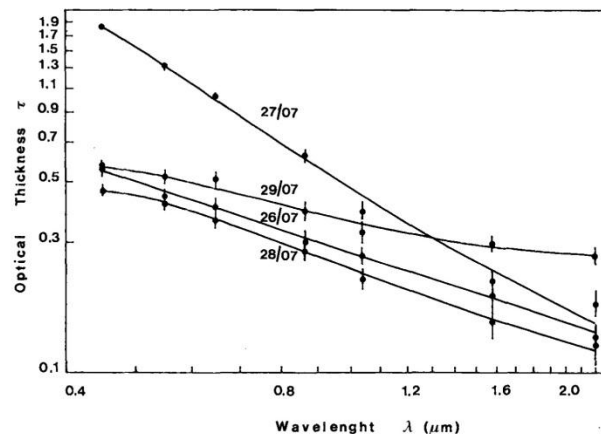


FIG. 2. Aerosol optical thickness as a function of the wavelength for the 4 days. The circles correspond to the measurements, and bars indicate the estimated errors. The solid lines represent the optical thickness spectral dependence computed with the retrieved size distribution.

Corresponding author address: Dr. J. L. Deuze, Laboratoire D'Optique Atmosphérique, Université Des Sciences Et Techniques De Lille, 59655 Villeneuve D'Ascq Cedex, France.

АКАДЕМИЯ НАУК СССР  
ТОМСКИЙ ФИЛИАЛ  
СИБИРСКОЕ ОТДЕЛЕНИЕ  
ИНСТИТУТ ОПТИКИ АТМОСФЕРЫ

Научный совет АН СССР по проблеме  
"Когерентная и нелинейная оптика"

Секция "Распространение оптических волн"  
Научного совета АН СССР по комплексной проблеме  
"Распространение радиоволн"

Уч. ВСЕСОЮЗНЫЙ СИМПОЗИУМ ПО ЛАЗЕРНОМУ И  
АКУСТИЧЕСКОМУ ЗОНДИРОВАНИЮ АТМОСФЕРЫ

Тезисы докладов  
(часть I)

Томск - 1984

- III -

УДК 551.593.5

РЕЗУЛЬТАТЫ ИЗМЕРЕНИЙ СПЕКТРАЛЬНОЙ ПРОЗРАЧНОСТИ  
АТМОСФЕРЫ В МОРСКИХ УСЛОВИЯХ

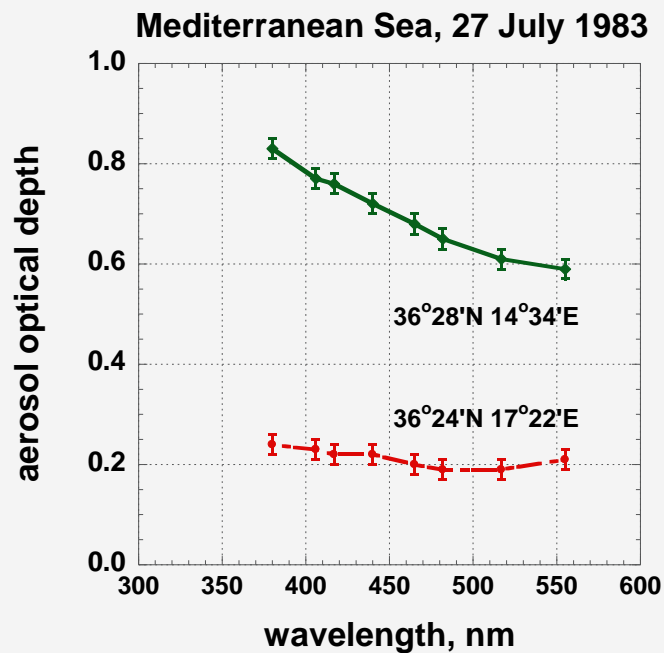
Ю.В.Виллевалде, К.С.Ламден, А.В.Смирнов

I. В последнее время в связи с задачами дистанционного зондирования океана с ИСЗ возрастает ценность экспериментальных данных

ных  
роз  
ких

том  
опи  
фил.  
луч  
при  
лас:  
вел  
го  
дни  
нак  
няле

тоне  
дли  
цию  
Расс  
ей с







2009/03/13